Fe-doping effects on the electrical and magnetic transitions in polycrystalline $Pr_{1-x}Sr_xMnO_3$ (x = 1/4, 3/8, and 1/2)

2004 J. Phys.: Condens. Matter 16 2839

(http://iopscience.iop.org/0953-8984/16/16/008)

INSTITUTE OF PHYSICS PUBLISHING JOURNAL OF PHYSICS: CONDENSED MATTER

J. Phys.: Condens. Matter **16** (2004) 2839–2847 PII: S0953-8984(04)69683-4

Fe-doping effects on the electrical and magnetic transitions in polycrystalline $Pr_{1-x}Sr_xMnO_3$ ($x = 1/4$, $3/8$, and $1/2$)

J Li[1,4], Z W Li[2], C K Ong[3] and D N Zheng[1]

[1] National Laboratory for Superconductivity, Institute of Physics, Chinese Academy of Sciences, Beijing 100080, People's Republic of China
[2] Temasek Laboratories, National University of Singapore, Engineering Drive 3, 119260, Singapore
[3] Centre for Superconducting and Magnetic Materials and Department of Physics, National University of Singapore, 2 Science Drive 3, 117542, Singapore

E-mail: lijie@ssc.iphy.ac.cn

Received 25 September 2003
Published 8 April 2004
Online at stacks.iop.org/JPhysCM/16/2839
DOI: 10.1088/0953-8984/16/16/008

Abstract

Electrical and magnetic transitions in $Pr_{1-x}Sr_xMnO_3$ and $Pr_{1-x}Sr_xMn_{0.95}Fe_{0.05}O_3$ ceramic samples with $x = 1/4$, $3/8$, and $1/2$ have been investigated. It is proved that 5% Fe doping in the system suppresses electrical conduction and ferromagnetism severely, but favours antiferromagnetism. The existence of spin clusters at temperatures above the ferromagnetic transition T_C is demonstrated in the Fe-doped $x = 1/2$ sample, which is caused by the Fe-doping-induced magnetic inhomogeneity. The transport behaviour above T_C in this sample is governed by variable-range hopping of the magnetic polarons. For the Fe-doped $x = 1/4$ sample, the insulator-to-metal (I–M) transition drops behind T_C by nearly 80 K; accordingly, two magnetoresistance peaks appear. One is around T_C, and the other lies just at the I–M transition temperature. The possible underlying mechanism is discussed qualitatively.

(Some figures in this article are in colour only in the electronic version)

1. Introduction

Distorted perovskite manganites $Ln^{3+}_{1-x}A^{2+}_xMnO_3$ (Ln—rare earth, A—alkaline earth) manifest a crucial dependence of their physical properties on the average A-site ion radii $\langle r_A \rangle$, other than the hole carrier density [1–4]. As is well known, when the A-site ions are too small to fill the cubes among MnO_6 octahedra, the octahedra will rotate and tilt inward to reduce

[4] Author to whom any correspondence should be addressed.

the excess space, leading to a Mn–O–Mn angle less than 180°. As a result, the overlap of the Mn and O electron orbitals is reduced; concomitantly, the conducting one-electron bandwidth W is narrowed [1, 3]. Therefore, for a given doping concentration 0.3, when $\langle r_A \rangle$ is changed from 1.12 to 1.30 Å, the insulator-to-metal (I–M) transition temperature T_ρ and the paramagnetic to ferromagnetic (PM–FM) transition temperature T_C both increase drastically, as well demonstrated by Hwang *et al* [1]. In the phase diagram they constructed, the nearly vertical boundary near $\langle r_A \rangle = 1.2$ Å is worthy of much attention. It is highly possible that more intriguing electrical and magnetic phase transitions will occur here if the thermodynamic conditions fluctuate only slightly. For compounds with commensurate doping concentrations such as 1/8, 1/3, and 1/2, antiferromagnetism (AFM) and charge/orbital ordering may also set in [2, 3], and 'complex behaviours' are expected in this region [4].

Among all the systems falling into this scope, $Pr_{1/2}Sr_{1/2}MnO_3$ ($\langle r_A \rangle = 1.22$ Å) is one of the most intriguing. Previous reports reveal that the system becomes an FM metal below $T_C = 250$ K, but transforms to an A-type instead of a CE-type AFM nonmetal at $T_N = 150$ K. The resistivity shows a steep increase at T_N, yet remains moderately low down to several kelvins. Neutron diffraction studies rule out charge ordering (CO) in the AFM/orbital ordering state of the system. This has been attributed to its nature of intermediate W [5–8]. Furthermore, it is also noted that in other systems with intermediate W, where the lattice distortion is minimal, existence of magnetic polarons has been confirmed by neutron scattering [9] or emission Mössbauer investigations [10]. It is argued that in these manganites a complex short-ranged magnetic ordering is coupled with the lattice distortion and governs the hopping-based electrical conduction far above T_C. It is then reasonable to suggest that in such kinds of system with intermediate W, the energy difference among various magnetic ground states is quite trivial, so it is feasible to tune their magnetic status by only slightly varying factors such as carrier doping, temperature, magnetic field, pressure, or Mn-site doping [11, 12].

On the other hand, the effects of iron doping in the Mn site have been widely probed in systems such as $La_{1-x}Pb_xMnO_3$ [13], $La_{1-x}Ca_xMnO_3$ [14, 15], and $La_{1-x}Sr_xMnO_3$ [16]. As far as we know, the Fe-doping effect on the specific $Pr_{1-x}Sr_xMnO_3$ system has not been fully investigated yet. Since the radius of Fe^{3+} is almost identical to that of Mn^{3+}, the introduction of Fe does not cause any appreciable distortion in the lattice [13, 16]. According to previous reports, however, the iron ions bring about an AFM superexchange interaction, and lead to a substantial decrease in the double exchange transfer integral [13]. Therefore, Fe doping may act to blur or shift the boundary in the phase diagram. In this paper we doped 5% Fe into a $Pr_{1-x}Sr_xMnO_3$ series with $x = 1/4$, 3/8, and 1/2, which corresponds to $\langle r_A \rangle = 1.18$, 1.20, and 1.22 Å, respectively, just spanning the boundary region. For comparison, a series of fully stoichiometric samples without Fe doping were also investigated. Direct evidence of the existence of spin clusters above T_C in the polycrystalline $Pr_{0.5}Sr_{0.5}Mn_{0.95}Fe_{0.05}O_3$ has been given.

2. Experimental details

$Pr_{1-x}Sr_xMnO_3$ (PSMO) and $Pr_{1-x}Sr_xMn_{0.95}Fe_{0.05}O_3$ (PSMFO) ceramic samples with $x = 1/4$, 3/8, and 1/2 were sintered by a conventional solid state reaction process at 1300 °C in air. The samples were bar shaped with dimensions around $3 \times 1 \times 10$ mm^3. Fine-step θ–2θ x-ray diffraction (XRD) was used to characterize the microstructure of the samples. At room temperature, the $x = 1/4$ and 3/8 samples show orthorhombic structure, while the $x = 1/2$ sample is tetragonal [7]. All the samples are single phase without detectable secondary phase or impurity. No structural change due to the Fe doping was observed from the diffraction spectra. The standard four-probe method was employed to evaluate the sample magnetoresistive properties. The measurements were carried out in zero field and 15 kOe over a temperature

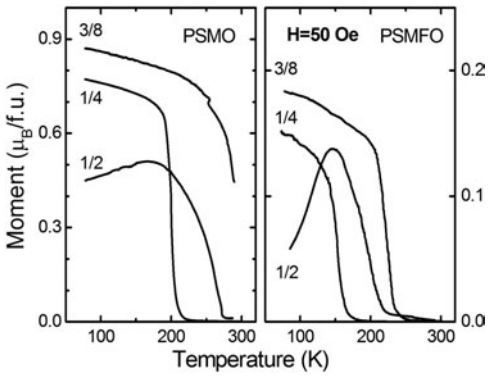

Figure 1. Temperature dependence of the magnetic moment per formula unit (fu) for the fully stoichiometric PSMO and the Fe-doped PSMFO with $x = 1/4$, 3/8, and 1/2, measured in a field of 50 Oe.

range of 78–325 K while cooling down and warming up, respectively. The ramp rate was kept at 3 K min^{-1}, and the accuracy of the temperature control was ± 0.1 K. The magnetic field was applied parallel to the current direction. The magnetic properties were probed using an Oxford superconducting vibrating-sample magnetometer (VSM), with the applied magnetic field along the sample longitude. The cooling rate was fixed at 5 K min^{-1} during the measurement of magnetization M versus temperature T curves. The dimension and mass for each sample were carefully checked to calculate the sample resistivity and magnetic moment.

3. Results

3.1. Magnetic properties

Figure 1 presents the temperature dependence of magnetic moment per formula unit for the PSMO and PSMFO series in a field of 50 Oe. For the undoped PSMO(1/4), there is a fairly sharp PM to FM transition occurring around 220 K. With increasing doping concentration and thus increasing carrier density, as in the case of $x = 3/8$, T_C rises to a higher temperature of about 320 K. When x is further increased to 1/2, however, T_C decreases again to 270 K due to the carrier localization effect. At lower temperatures an AFM ordering appears in the $x = 1/2$ sample, which is characterized by a decline of the magnetic moment, though T_N cannot be well defined from the curve. We noted that, in contrast to published data [8], in our $x = 1/2$ sample the magnetization is not completely suppressed at low temperatures. This is most probably due to a slight Sr deficiency in our sample, originating from the moist starting materials. It has been demonstrated that around $x = 1/2$ even a tiny off-stoichiometry can cause drastic changes in the magnetic and transport properties [17]. But this deficiency should have little effect on the contrast between the Fe-doped and undoped samples. The FM transition in the Fe-doped PSMFO series follows the same law, but the T_C all shift to lower temperatures. For PSMFO(1/4), as an example, T_C is only around 180 K, 40 K lower than its undoped partner. Meanwhile, the magnetic moment for PSMFO(1/2) goes down steeply at low temperatures, suggesting a sharper FM–AFM transition and subsequently a narrower temperature range for the FM state. Moreover, noting the different vertical scales for the two panels, it is obvious that the ferromagnetic coupling is greatly suppressed in the Fe-doped system.

Magnetization curves measured at 77 K in a field up to 50 kOe for the six samples are shown in figure 2. The saturation magnetic moment per formula unit (μ_S) can be estimated using the

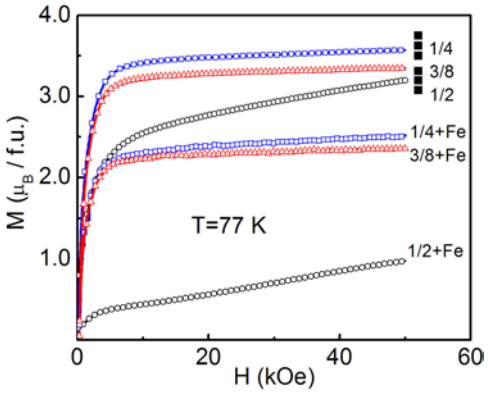

Figure 2. Magnetization curves for the PSMO and the Fe-doped PSMFO with $x = 1/4$, $3/8$, and $1/2$, measured at 77 K in a field up to 50 kOe. The calculated values of saturation moment per formula unit (μ_S) are denoted by filled squares.

simple single-ion model. The spin moments at 0 K for Mn^{3+}, Mn^{4+}, and Fe^{3+} are 4, 3, and 5 μ_B, respectively. According to neutron diffraction results, in the $Pr_{0.7}Ca_{0.3}MnO_3$ compound Pr ions show a moment of 0.45 μ_B only at temperatures below 60 K [18]. Therefore, here we ignore the moment of Pr^{3+} in our system and calculate μ_S by assuming an FM arrangement among Mn ions and an AFM arrangement between the Mn and Fe ions [16]. The calculated μ_S at 0 K for each sample is denoted in the right-hand side of the figure by filled squares. We can see that the experimental data for the PSMO samples with $x = 1/4$ and $3/8$ (3.58, 3.35 μ_B/fu) are close to the theoretical values (3.75, 3.63 μ_B/fu), which reveals that in the two samples Mn^{3+} and Mn^{4+} ions are fully ferromagnetically coupled. The small difference may be because the data were recorded at 77 K instead of 0 K. The PSMO(1/2) sample shows a slightly lower saturation moment but a large high-field susceptibility χ, suggesting that in this sample an AFM ordering is superimposed on the FM ordering. Here the residual FM ordering may be attributed to a slight Sr deficiency in the sample, as mentioned above. With Fe doping, the PSMFO samples with $x = 1/4$ and $3/8$ reach their saturation moments (2.50, 2.35 μ_B/fu) in a fairly low field, but these values are far below theoretical predictions (3.31, 3.20 μ_B/fu). This indicates that in these samples not only are the Fe ions antiferromagnetically aligned with Mn ions, but also the FM coupling among Mn^{3+} and Mn^{4+} ions is severely weakened [13]. The PSMFO(1/2) sample shows a very low remanent moment, yet exhibits a high-field χ similar to its undoped partner. This suggests that the FM ordering almost diminishes in the sample, which is evidence that Fe doping stabilizes the AFM state [14].

The field dependence of magnetization (M–H) for the six samples was investigated at room temperature. While the other samples show typical paramagnetic behaviour above T_C, the Fe-doped PSMFO(1/2) exhibits anomalous behaviour, as presented in figure 3. At 300 K, far above its ferromagnetic transition point (220 K), the sample demonstrates a small but clear hysteresis in a field within $\pm$3000 Oe, while showing a conventional linear dependence at fields beyond. We again measured the same sample at reduced temperatures (280, 260, and 240 K) and the curves recorded are all plotted in the same panel. With decreasing temperature, as clearly presented in the zoom-in inset in fourth quadrant, the 'saturated' magnetization of the hystereses increases, while the coercivity field ($\sim$500 Oe) is almost unchanged. The high-field χ also grows gradually with decreasing temperature. Comparing the curve with that of the undoped PSMO(1/2) measured at 77 K, the 'saturated' magnetizations for the small loops are

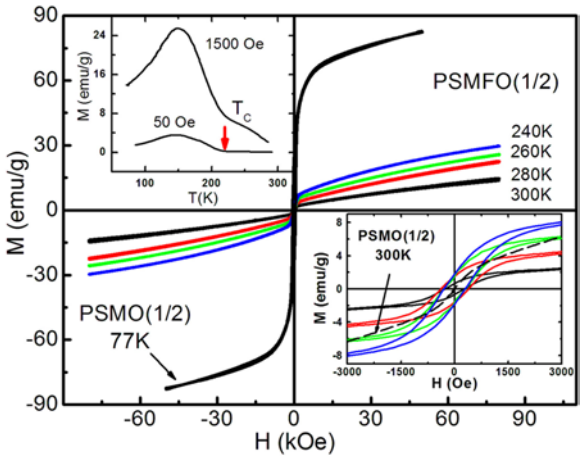

Figure 3. Small magnetization hysteresis observed at temperatures above T_C for the Fe-doped PSMFO(1/2) sample. For comparison, the loop at 77 K for the undoped partner PSMO(1/2) is also plotted. Inset in the fourth quadrant is the zoom-in of the low-field region. The dashed curve is the M–H curve at 300 K for the undoped partner. The inset in the second quadrant shows the M–T curve of the sample measured in 50 and 1500 Oe upon cooling.

quite low, only about one-tenth of that in the former, and the coercivity field is also lower. The M–H curve at 300 K of the undoped PSMO(1/2), also plotted in the inset by a dashed curve, strictly shows no hysteresis. This excludes the possibility of pseudo results by our experimental set-up. In order to reveal the underlying mechanism, we re-measured the M–T curve of the ion-doped sample in a higher field of 1500 Oe. The result is shown in the inset in the second quadrant of the figure. Comparing the two curves measured in different fields we find that there is a field-induced magnetization above T_C in a quite large temperature range from 300 to 220 K. We then argue that small clusters with short-ranged magnetic ordering exist in the paramagnetic matrix, which can easily rotate in a fairly low magnetic field, and grow and coalesce when the temperature is reduced.

We have collected Mössbauer spectra for all PSMFO samples from room temperature to 4.2 K. The spectra at 4.2 K have hyperfine fields of 490 kOe and quadrupole splittings of zero. However, the hyperfine field is about 340 kOe for metal Fe, and the hyperfine field is about 540 kOe as well as the quadrupole splitting being about 0.3–0.4 mm s^{-1} for α-Fe_2O_3. Therefore, based on Mössbauer parameters, Fe clusters in PSMFO can be fully ruled out, and the spin clusters in PSMFO(1/2) observed above T_C are a new phenomenon that can be solely attributed to Fe doping. An instinctive explanation is that the Fe doping brings magnetic inhomogeneity into the system, thus favouring the formation of spin clusters.

3.2. Magnetoresistive properties

Figure 4(a) is the ρ–T curves for the undoped series in zero field (solid curves) and 15 kOe (dash curves). T_C obtained from M–T measurements are indicated in this figure by arrows. The transport properties in these undoped samples are well consistent with their magnetic characterizations. The inflexion of the curves locates just around T_C, complying with the framework of double exchange (DE). While samples $x = 1/4$ and 3/8 are metal below T_C, for $x = 1/2$ the I–M transition at $T_C \sim 270$ K and the steep resistivity rise at $T_N \sim 160$ K, as previously demonstrated [5], are absent in the present sample. It shows insulator-like behaviour

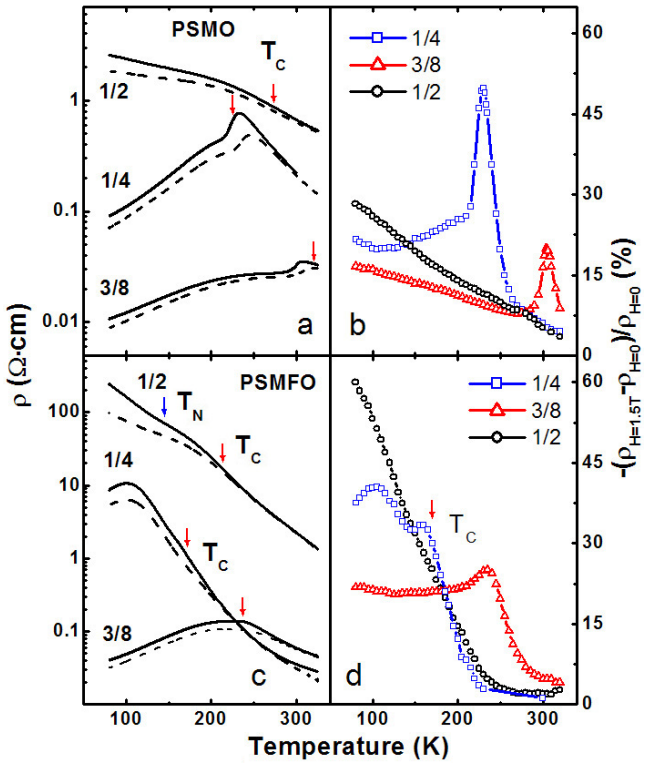

Figure 4. ρ–T curves for the undoped PSMO series (a), and the Fe-doped PSMFO series (c) in zero field (solid curves) and 15 kOe (dashed curves), and the derived MR–T curves for the PSMO series (b) and the PSMFO series (d). Arrows indicate T_C or T_N defined from the M–T curves.

in the whole temperature range with a resistivity bump around T_N, and ρ reaches a fairly high value at low temperatures due to the AFM and orbital ordering. The apparent difference may be attributed to the extremely large resistivity anisotropy in PSMO(1/2) below T_N [19], the grain boundaries in polycrystalline samples [20, 21], and most importantly the slight Sr deficiency. The derived MR ratios, defined as $(\rho_{H=1.5\ \mathrm{T}} - \rho_{H=0})/\rho_{H=0}$, are presented in figure 4(b). For samples $x = 1/4$ and 3/8, the MR ratio has a maximum near T_C, and decreases fast as the temperature deviates from this value. The peak amplitude also declines with increasing x. The ratio rises again at low temperatures due to the spin-dependent scattering at grain boundaries. For the $x = 1/2$ sample, the peak near T_C is suppressed and broadened, and at low temperatures the MR ratio increases rapidly, reaching a fairly large value. This can be attributed to the canting of the originally antiparallel spins in a magnetic field as well as the spin-dependent scattering.

ρ–T curves for the Fe-doped series in zero field (solid curves) and 15 kOe (dashed curves) are presented in figure 4(c). T_C for all the Fe-doped samples, and T_N (defined as the summit of the M–T curve) for sample PSMFO(1/2) are indicated. Comparing with figure 4(a) one can see that resistivities for the Fe-doped samples are one to two orders of magnitude higher than that for the undoped samples. Moreover, it is clear that Fe doping not only severely suppresses the PM–FM transition, but also pushes the I–M transition T_ρ to lower temperatures. We also note that for the sample PSMFO(1/4) T_ρ is only around 100 K, about 80 K lower than its T_C. This is obviously beyond the framework of DE. MR–T curves for the Fe-doped series

also show features different from their partners, as shown in figure 4(d). For PSMFO(3/8), the MR peak around T_C remains, but is considerably broadened due to the inhomogeneity introduced by Fe doping. Its MR ratio is slightly enhanced. We also find the MR–T curve interesting for the $x = 1/2$ sample, referring to the unusual magnetic properties observed above T_C—spin clusters. For this sample, at liquid nitrogen temperature the MR ratio is as high as 60%, twice that of its undoped partner, but within the temperature range 220–300 K it is very close to zero. This is consistent with our previous deduction that in this sample the conducting behaviour above T_C is governed by magnetic polarons, which are carriers bound to lattice distortions coupled with short-ranged ferromagnetic ordering. Applying a magnetic field will not affect the local environment for each carrier, i.e., the field cannot alter the binding energy of the polarons, and therefore the resistivity drop in the presence of a field is quite limited. Furthermore, a more striking two-peak feature is observed in the curve for sample PSMFO(1/4). The conventional peak is at a temperature slightly below T_C, while the other one lies just where the I–M transition occurs. With a careful survey of the corresponding ρ–T curve we also find an inconspicuous bump at T_C. This two-peak feature in the Fe-doped polycrystalline samples has been observed previously in other systems [22], and the possible reasons behind this will be discussed in the next section.

4. Discussions

It is well known that DE between Mn^{3+} and Mn^{4+} ions accounts for the ferromagnetism and metallic conduction in the manganites. The doped iron substitutes Mn^{3+} in the perovskite lattice, and exists as Fe^{3+} [13]; as a result, doping reduces the number of Mn^{3+}–Mn^{4+} pairs in the samples. On the other hand, according to Ahn *et al* [14], the top of the Fe e_g band locates almost at the bottom of Mn e_g band, with just an overlap of less than 3%. Therefore, Fe^{3+} cannot effectively participate in the DE process; in contrast, the B-site now occupied by Fe^{3+} blocks the conducting patch. Moreover, Fe doping induces the Mn spin canting, and thus reduces the DE transfer integral. For the above reasons, Fe doping favours insulating and AFM behaviour, as evidenced by our experimental results.

Apparently, the Fe doping introduces randomly distributed energy barriers in the system, so that the transport behaviour above the I–M transition is governed by the variable-range hopping (VRH) of polarons [23, 24]: $\rho = \rho_\infty \exp[(T_0/T)^{1/4}]$, where $kT_0 = 18\alpha^3/N(E)$ and α is the polaron hopping distance. We fitted the ρ–T curves of the Fe-doped samples using the VRH model. For sample PSMFO(1/4), although the insulating behaviour dominates in a temperature range 100–300 K, the curve cannot be well fitted using one single pair of parameters. On the contrary, it can only be fitted by two straight lines crossed at T_C, as shown in figure 5. Assuming that the density of states in this sample does not change, from the fitting parameter T_0 we can obtain the ratio of the localization length $(1/\alpha)$ for the two segments. It is found that $1/\alpha$ above T_C is 1.2 times that below T_C. This means the hopping distance is longer or the resistivity is smaller after the long-range FM ordering is established, which is the reason for the small MR peak at T_C. That is, in a temperature range below T_C (170–100 K), the sample behaves as an FM insulator and its conduction follows the VRH model, similar to the case of very small $\langle r_A \rangle$ [1]. In fact, Raman studies also suggest magnetic polarons in this doping concentration [24]. Then it is reasonable to suggest that Fe doping further reduces W in the sample. A metallic behaviour can only start to manifest itself as the temperature is further reduced. A magnetic field can also right-shift the I–M transition, causing the second MR peak. In contrast, the Fe-doped $x = 3/8$ sample undergoes the I–M and PM–FM transitions almost simultaneously due to its relatively higher carrier density and larger W.

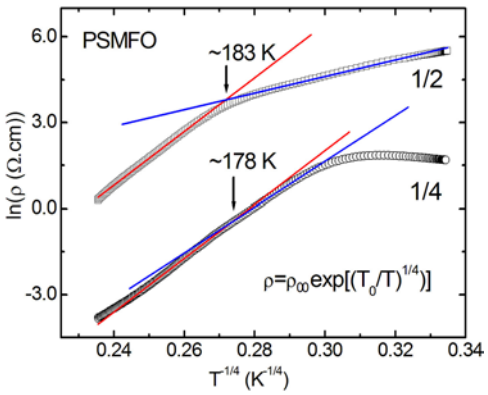

Figure 5. Fitting results of the ρ–T curves for PSMFO samples with $x = 1/4$, and $1/2$ using the VRH model. T_0 and ρ_∞ are the fitting parameters.

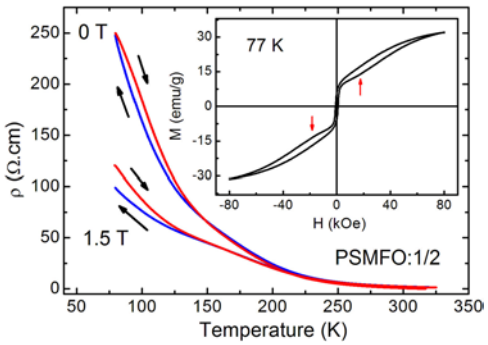

Figure 6. Thermal hysteresis in the ρ–T curves for the sample PSMFO(1/2). Inset is the magnetization loop for this sample measured at 77 K.

As $x = 1/2$, a commensurate value, in the Fe-doped sample the I–M transition is absent. Taking advantage of the Fe-doping-induced magnetic inhomogeneity, magnetic polarons instead of small polarons appear at high temperatures, as clearly revealed by the small hysteresis loops above T_C. The VRH fitting of the ρ–T curve for this sample can also be divided into two segments. The slopes for the two straight lines are greatly different, suggesting that a structure transition occurs here at ~180 K. This is coincident with the transition from tetragonal $I4/mm$ to orthorhombic $Fmmm$ symmetry, associated with the AFM transition [7]. As shown in figure 6, thermal hystereses are observed at low temperatures, revealing the first-order nature of this transition. If it is correct that doping Fe ions into Mn sites suppresses the conducting bandwidth W, a CO transition may also occur at T_N in the PSMFO(1/2) sample. An indirect evidence of this CO state is given in the inset of figure 6. We can see from the loop that the magnetization tends to be saturated around 1 T, but starts to rise faster when the field is higher than 2 T. This is a sign of a metamagnetic transformation [17]. It can be a partial melting of the CO state in a magnetic field. This can also explain the drastically increased resistivity and the very large MR ratio at low temperatures for this sample. Nevertheless, most probably the Sr deficiency which happens in the undoped $x = 1/2$ sample also occurs in this Fe-doped sample; therefore, the merit of our discussion above is weakened to some extent.

5. Conclusions

In conclusion, as compared to the undoped sample, 5% Fe doping into the $Pr_{1-x}Sr_xMnO_3$ system severely impairs the DE process and reduces T_C and T_ρ. The insulating and AFM state are then stabilized. Small magnetic hystereses were observed in the Fe-doped sample with $x = 1/2$ at temperatures well above T_C. This is direct evidence that spin clusters with short-ranged FM order exist in the sample due to the Fe-doping-induced magnetic inhomogeneity. The I–M transition in the doped sample PSMFO(1/4) is far behind its PM–FM transition, and accordingly two MR peaks appear at T_C and T_ρ respectively. The FM insulating state in this sample is attributed to the further reduction in bandwidth W by Fe doping.

Acknowledgments

We acknowledge partial financial support by the National Natural Science Foundation of China under grant No 10174093, and the Ministry of Science and Technology under grant No NKBRSF-G19990646. One of the authors, JL, would like to thank Dr K Chen and Mr J Y Xiang for their helpful discussions.

References

[1] Hwang H Y, Cheong S-W, Radaelli P G, Marezio M and Batlogg B 1995 *Phys. Rev. Lett.* **75** 914
[2] Rao C N R and Raveau B 1998 *Colossal Magnetoresistance, Charge Ordering and Related Properties of Manganese Oxides* (Singapore: World Scientific)
[3] Arulraj A, Santhosh P N, Gopalan R S, Guha A, Raychaudhuri A K, Kumar N and Rao C N R 1998 *J. Phys.: Condens. Matter* **10** 8497
[4] Arulraj A, Gundakaram R, Biswas A, Gayathri N, Raychaudhuri A K and Rao C N R 1998 *J. Phys.: Condens. Matter* **10** 4447
[5] Kawano H, Kajimoto R, Yoshizawa H, Tomioka Y, Kuwahara H and Tokura Y 1997 *Phys. Rev. Lett.* **78** 4253
[6] Yoshizawa H, Kawano H, Fernandez-Baca J A, Kuwahara H and Tokura Y 1998 *Phys. Rev.* B **58** R571
[7] Pollert E, Jirák Z, Hejtmánek J, Strejc A, Kužel R and Hardy V 2002 *J. Magn. Magn. Mater.* **246** 290
[8] Llobet A, Carcía-Muñoz J L, Frontera C and Ritter C 1999 *Phys. Rev.* B **60** R9889
Raveau B, Hervieu M and Maignan A 1999 *Phys. Rev.* B **62** 6820
[9] Kusters R M, Singleton J, Keen D A, McGreevy R and Hayes W 1998 *Physica* B **155** 362
[10] Chechersky V, Nath A, Isaac I, Franck J P, Ghosh K and Greene R L 2001 *Phys. Rev.* B **63** 052411
[11] Damay F, Maignan A, Martin C and Raveau B 1997 *J. Appl. Phys.* **82** 1485
[12] Barnabé A, Margnan A, Hervieu M, Damay F, Martin C and Raveau B 1997 *Appl. Phys. Lett.* **71** 3907
[13] Leung L K, Morrish A H and Evans B J 1976 *Phys. Rev.* B **13** 4069
[14] Ahn K H, Wu X W, Liu K and Chien C L 1996 *Phys. Rev.* B **54** 15299
[15] Righi L, Gorria P, Insausti M, Gutiérrez J and Barandiarán J M 1997 *J. Appl. Phys.* **81** 5767
[16] Huang Q, Li Z W, Li J and Ong C K 2001 *J. Phys.: Condens. Matter* **103** 4033
[17] Hejtmánek J, Pollert E, Jirák Z, Sedmidubský D, Strejc A, Maignan A, Martin Ch, Hardy V, Kužel R and Tomioka Y 2002 *Phys. Rev.* B **66** 014426
[18] Cox D E, Radaelli P G, Marezio M and Cheong S-W 1998 *Phys. Rev.* B **57** 3305
[19] Kuwahara H, Okuda T, Tomioka Y, Asamitsu A and Tokura Y 1999 *Appl. Phys. Lett.* **82** 4316
[20] Knížek K, Jirák Z, Pollert E, Zounová F and Vratislav S 1992 *J. Solid State Chem.* **100** 292
[21] Li J, Ong C K, Zhan Q and Li D X 2002 *J. Phys.: Condens. Matter* **14** 6341
[22] Xianyu W X, Li B H, Qian Z N and Jin H M 1999 *J. Appl. Phys.* **86** 5164
[23] Viret M, Ranno L and Coey J M D 1997 *J. Appl. Phys.* **81** 4964
[24] Liu J-M, Yu T, Huang Q, Li J, Shen Z X and Ong C K 2002 *J. Phys.: Condens. Matter* **14** L141